Specific heat, susceptibility, magnetotransport and thermoelectric power of the Kondo alloys $(Ce_{1-x}La_x)Cu_5In$

2004 J. Phys.: Condens. Matter 16 1981

(http://iopscience.iop.org/0953-8984/16/12/007)

INSTITUTE OF PHYSICS PUBLISHING JOURNAL OF PHYSICS: CONDENSED MATTER

J. Phys.: Condens. Matter **16** (2004) 1981–1994 PII: S0953-8984(04)68634-6

Specific heat, susceptibility, magnetotransport and thermoelectric power of the Kondo alloys $(Ce_{1-x}La_x)Cu_5In$

M B Tchoula Tchokonté[1], P de V du Plessis[1], A M Strydom[2], D Kaczorowski[3], A Czopnik[3] and Z Kletowski[3]

[1] f-Electron Magnetism and Heavy-Fermion Physics Research Programme, School of Physics, University of the Witwatersrand, Private Bag 3, PO Wits 2050, Johannesburg, South Africa
[2] Department of Physics, Rand Afrikaans University, Johannesburg, South Africa
[3] Institute of Low Temperature and Structure Research, Polish Academy of Sciences, PO Box 1410, 50-950 Wrocław, Poland

E-mail: ams@na.rau.ac.za

Received 5 September 2003
Published 12 March 2004
Online at stacks.iop.org/JPhysCM/16/1981 (DOI: 10.1088/0953-8984/16/12/007)

Abstract

The influence of substituting Ce with La in the Kondo compound $CeCu_5In$ has been investigated using x-ray diffraction, specific heat (C_p), electrical resistivity ($\rho(T)$), magnetoresistivity (MR) and thermoelectric power (TEP) measurements. C_p of $CeCu_5In$ and the $(Ce_{1-x}La_x)Cu_5In$ alloys shows enhanced values at low temperatures. Between 10 and 20 K the equation $C_p/T = \gamma^{\rm conv} + \beta T^2$ fits the data for all alloys with $\gamma^{\rm conv}$ scaling linearly with Ce concentration. Below 10 K a pronounced upturn in C_p values occurs. Susceptibility data above 100 K follow the Curie–Weiss relation and give effective moment $\mu_{\rm eff}$ values in fair agreement with that of a Ce^{3+}-ion. The $\rho(T)$ studies illustrate the evolution from Kondo lattice to single-ion Kondo behaviour with increase in La content in the $(Ce_{1-x}La_x)Cu_5In$ alloy series. MR measurements on Ce dilute alloys are interpreted within the single-ion Bethe ansatz description and values of the Kondo temperature $T_{\rm K}$ are calculated. A compressible Kondo lattice model has been used to describe the decrease in $T_{\rm K}$ and in $T_{\rm m}^{\rho}$ (the temperature at which a maximum in $\rho(T)$ occurs for the coherent dense Kondo alloys) with decrease in Ce concentration for these alloys. The TEP is positive and shows a maximum at approximately 45 K for several investigated $(Ce_{1-x}La_x)Cu_5In$ alloys.

1. Introduction

Many studies have been devoted to the thermodynamic and transport properties of the heavy-fermion compound $CeCu_6$ [1]. Doping experiments on $CeCu_6$ have also received

considerable attention. In one group of studies Ce has been replaced by non-magnetic La, Y or Th or by moment-bearing rare-earth ions Gd, Tb, Pr or Nd [2]. In another series of experiments Cu has been replaced by M = Au, Ag or Pd. This leads to antiferromagnetic ordering for the $Ce(Cu_{6-x}M_x)$ alloys above a critical concentration x_c at which the Rudermann–Kittel–Kasuya–Yosida interaction dominates the Kondo interaction. $Ce(Cu_{6-x}Au_x)$ samples of the critical concentration $x_c = 0.1$ have been studied extensively and shown to exhibit non-Fermi liquid behaviour [3]. Transport studies on $CeCu_6$ indicate the occurrence of a peak in the resistivity $\rho(T)$ at ∼10 K, below which it drops rapidly [4]. Coherent Fermi-liquid behaviour characterized by a T^2-dependence of $\rho(T)$ is only attained below 100 mK [4–6].

Kasaya *et al* [7] reported the existence of the $CeCu_5In$ compound which has the same orthorhombic *Pnma* crystal structure as $CeCu_6$. The replacement of a Cu atom with In yields a Kondo lattice compound for which $\rho(T)$ has a well-defined peak at ∼35 K. Its coherent regime is considerably expanded compared to $CeCu_6$, as evidenced by a $\rho(T) \sim T^2$ Fermi liquid-like dependence between 0.1 and 4.5 K. The specific heat C_p of $CeCu_5In$ is less enhanced at low temperature than that of $CeCu_6$, as exemplified by a γ value of 200 mJ mol^{-1} K^{-2} for $CeCu_5In$ [7] compared to 1500 mJ mol^{-1} K^{-2} for $CeCu_6$ [4]. No evidence of magnetic order in $CeCu_5In$ has been found down to 0.1 K [7]. The Kondo behaviour has also been studied for $CeCu_{6-x}In_x$ alloys ($0.5 \leqslant x \leqslant 1.6$) [7, 8] and for $CeCu_5In_{1-x}M_x$ (M = Al or Ga) alloys [9].

The effects of replacing Ce with La in the dense Kondo compound $CeCu_5In$ are reported in the present paper. Results are presented of lattice parameter, specific heat, magnetic susceptibility, resistivity, magnetoresistivity and thermoelectric power measurements. The evolution from Kondo lattice to incoherent single-ion Kondo behaviour with increased La doping will be demonstrated. Values for the Kondo temperature T_K of the different $(Ce_{1-x}La_x)Cu_5In$ alloys are evaluated from our results, and their dependence on x and hence volume is discussed in terms of a compressible Kondo lattice model [10].

2. Experimental details

Polycrystalline samples of $(Ce_{1-x}La_x)Cu_5In$ were prepared by arc-melting the constituent elements on a water-cooled copper hearth in a titanium gettered argon atmosphere. Metals of the following purity in wt% were used: Ce, 99.98; La, 99.99; In and Cu, 99.999. Buttons were turned over and remelted several times to ensure good homogeneity of the samples. Weight losses after final melting were always smaller than 1%. One part of each arc-melted button was subsequently wrapped in Ta foil and annealed in an argon atmosphere in a quartz tube for 10 days at a temperature of 850 °C. Measurements were performed on as-cast or annealed samples as indicated in section 3.

Room-temperature x-ray powder diffraction spectra of all compounds prepared in the $(Ce_{1-x}La_x)Cu_5In$ series could be indexed according to the orthorhombic *Pnma* crystal structure. No evidence of parasitic phases or unreacted elements was found in the x-ray spectra. Individual peak positions were determined using the WINPLOTR program for powder diffraction, Beta Version/LLB-February 1999. The results were used to calculate lattice parameters through a least-squares (LSQ) fit of 15 well-resolved diffraction lines using the UnitCell program [11].

Magnetization measurements were performed on a single piece (∼10 mg mass) of each polycrystalline sample in the temperature range 1.7–300 K. A Quantum Design MPMS-5 SQUID magnetometer was used in fields up to 5 T. Specific heat measurements were performed in the temperature range 2.5–70 K by an automated adiabatic heat pulse calorimeter.

For electrical transport measurements, bar-shaped specimens of typical dimensions $1 \times 1 \times 8$ mm^3 were cut by spark-erosion from the sample ingots. A four-probe dc method

was used in these studies. Gold contact wires were spot-welded onto the specimens. Current-reversal was used to correct for possible thermal voltages in the circuitry. Magnetoresistance measurements were made using an Oxford Instruments variable temperature insert fitted into a Dewar that housed an 8 T superconducting solenoid. The electrical resistivity values $\rho(T)$ reported in this paper were typically measured to a sensitivity of 1 part in 1000. However, an absolute error of $\rho(T) \pm 2\%$ is estimated due to an uncertainty in geometrical factors. A further uncertainty could originate from the presence of microcracks in the sample, but the influence of these is difficult to quantify.

Thermoelectric power measurements were performed using a modified version of the equipment described by Henkie *et al* [12]. The bar-shaped sample was placed between two reference blocks of an $Ag_{97}Au_3$ alloy [13]. Electrical and thermal contacts between the sample and blocks were enhanced by wetting the contacts with a liquid In–Ga alloy. A temperature gradient of 1.5 K was maintained between the blocks while the sample temperature was swept at a rate of 18 K h^{-1} in the range 5–317 K.

3. Results and discussion

3.1. Lattice parameters and unit cell volume

The orthorhombic lattice parameters, as well as the unit cell volume, as obtained from analyses of the x-ray powder diffraction patterns for the various alloys are depicted in figure 1 as a function of x. A Vegard's rule linear increase in the unit cell volume with x is observed between $CeCu_5In$ and $LaCu_5In$.

3.2. Specific heat

Measurements of the specific heat C_p of the $(Ce_{1-x}La_x)Cu_5In$ series are depicted in figure 2 in the conventional C_p/T versus T^2 presentation. These measurements were performed on annealed samples. For all investigated Ce containing alloys the data between 10 and 20 K could be fitted to the conventional equation for the specific heat C_p of a metal at low temperatures:

$$C_p/T = \gamma^{\text{conv}} + \beta T^2 \tag{1}$$

with γ^{conv} and β referring respectively to the electronic and phonon contributions. For the reference compound $LaCu_5In$, the data conform to (1) down to low temperatures, with a small value of the electronic contribution to C_p as is to be expected, $\gamma^{\text{conv}} = 3.4$ mJ mol^{-1} K^{-2}. Values of γ^{conv} and β as obtained from an LSQ fit of (1) to the experimental data are given in table 1. It is observed that the γ^{conv} values of the Ce containing alloys are appreciably enhanced compared to that of the reference compound. Also in table 1 are values of the Debye temperature θ_D for the different alloys obtained from the relation

$$\theta_D = (12R\pi^4 n/5\beta)^{1/3} \tag{2}$$

where R is the gas constant and n is the number of atoms in a formula unit.

In all of the alloys studied, no evidence of a phase transition was observed down to the lowest measuring temperature of 2.5 K in the specific heat experiments. At lower temperatures, the Ce-containing alloys exhibit a pronounced upturn in their C_p/T values. This is to be interpreted as due to the onset of heavy-fermion (HF) behaviour with $\gamma = (C_p/T)_{T\to 0}$ values that are appreciably larger than the γ^{conv} values derived from the linear fits of (1) to the higher temperature data. In the inset to figure 2 it is shown that γ^{conv} scales linearly with Ce concentration. This illustrates the single-ion character of the Kondo behaviour as manifested in the specific heat for the temperature region $10 \leqslant T \leqslant 20$ K.

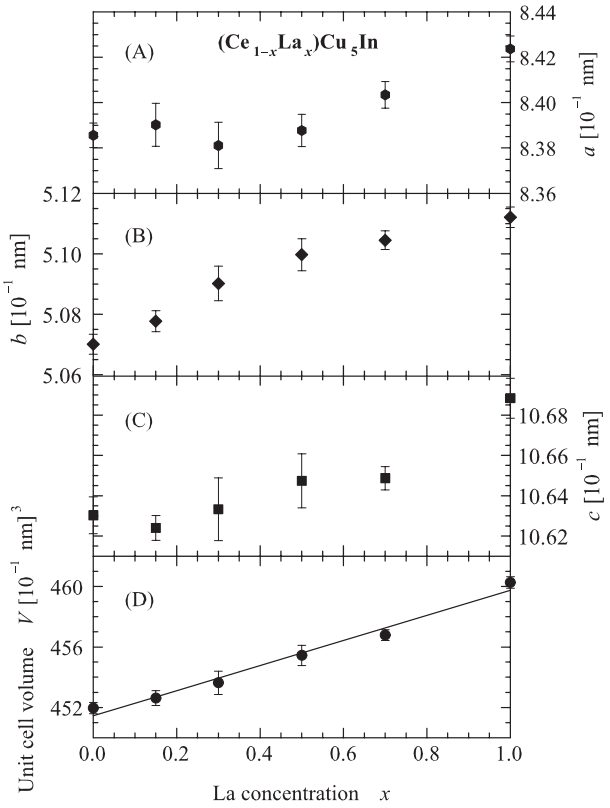

Figure 1. Lattice parameters (A) a, (B) b, (C) c and (D) unit cell volume V of the orthorhombic $(Ce_{1-x}La_x)Cu_5In$ alloy system.

Table 1. Values of the fit parameters γ^{conv} and β of the specific heat (see (1)) and the Debye temperature θ_D (see (2)) for several $(Ce_{1-x}La_x)Cu_5In$ alloys.

Ce concentration $(1-x)$	γ^{conv} (mJ mol^{-1} K^{-2})	β (mJ mol^{-1} K^{-4})	θ_D (K)
1	205(1)	0.98(1)	240(1)
0.9	187(3)	0.96(1)	243(1)
0.8	168(2)	0.95(2)	243(2)
0.6	113(2)	0.99(1)	240(1)
0.4	83(2)	1.10(1)	231(1)
0.2	43(2)	1.18(2)	226(1)
0	3.4(5)	1.18(1)	226(2)

The upturn in C_p/T observed at low temperatures in figure 2 is characteristic of many HF and moderate HF compounds [14]. In the case of HF UPt_3 it was shown that by adding a term characteristic of spin-fluctuations to the conventional equation, an appropriate description of its $C_p(T)$ could be obtained [15]. An expression for the temperature dependence of the spin-fluctuation contribution to the specific heat was initially derived by Doniach and Engelsberg [16], and its presence was observed in the spin-fluctuation system UAl_2 [17, 18]. This concept was, however, unsuccessful in describing the rapid rise in C_p/T at low temperatures in other HF compounds such as $CeCu_2Si_2$, UBe_{13}, $NpBe_{13}$, $CeAl_3$ and $CeCu_6$ [14].

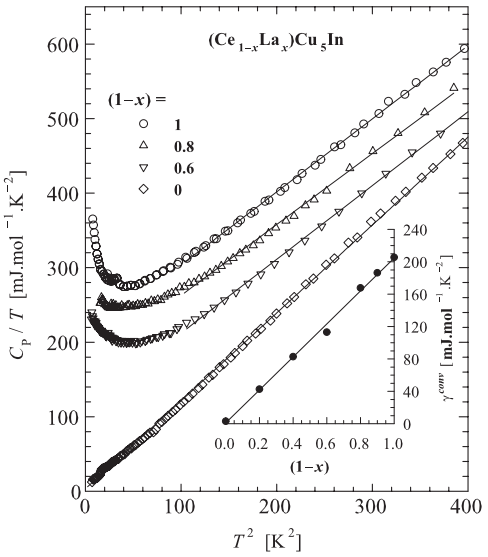

Figure 2. The temperature variation of the heat capacity C_p/T in the range $2 \leqslant T \leqslant 20$ K for alloys of $(Ce_{1-x}La_x)Cu_5In$ with $(1-x) = 0$, 0.6, 0.8 and 1. The solid curves are LSQ fits of $C_p/T = \gamma^{conv} + \beta T^2$ to the data. The inset shows how γ^{conv} as derived from the measurements taken at higher temperatures scales with Ce concentration $(1-x)$.

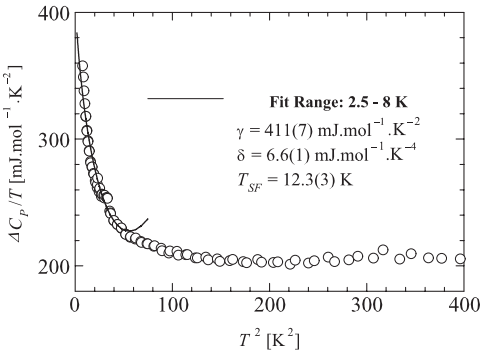

Figure 3. A plot of $(\Delta C_p/T)_{CeCu_5In} = (C_p/T)_{CeCu_5In} - \beta T^2$ versus T^2 showing a fit of (3), which includes a spin-fluctuation term, to the data.

To better facilitate comparison of the low-temperature data of $CeCu_5In$ with a spin-fluctuation description, its phonon contribution as given by βT^2 with $\beta = 0.98$ mJ mol^{-1} K^{-4} was subtracted from the experimental C_p/T data for the compound to give $(\Delta C_p/T)_{CeCu_5In} = (C_p/T)_{CeCu_5In} - \beta T^2$. A fit of $(\Delta C_p/T)$ to a spin-fluctuation description

$$\Delta C_p/T = \gamma + \delta T^2 \ln(T/T_{SF}) \tag{3}$$

for the temperature range 2.5–8 K is given in figure 3, together with the fit parameters γ, δ, and the spin-fluctuation temperature T_{SF}. At higher temperatures the data in figure 3 conform with the temperature-independent value $(\Delta C_p/T) \simeq \gamma^{conv}$.

3.3. Magnetic susceptibility

The magnetic field dependence of the magnetization $\sigma(\mu_0 H)$ measured at 1.7 K is shown in figure 4 for some representative members of the $(Ce_{1-x}La_x)Cu_5In$ series, namely for the $1-x = 0.6$, 0.8 and 1 alloys. Magnetization and susceptibility measurements reported in this section were made on annealed samples. In a few instances we also performed measurements on the corresponding as-cast alloys, and observed results that generally agree with those obtained on the annealed samples. For all alloys σ exhibits a linear field dependence except for a small downwards curvature at the highest fields. There is no evidence of any hysteresis during the process of increasing and decreasing of the field. Results of susceptibility $\chi(T)$ measurements taken in a field of 0.1 T are depicted for the $1-x = 0.6$, 0.8 and 1 alloys in figure 5, together with the inverse susceptibility $\chi^{-1}(T)$. For temperatures above 100 K the results follow a

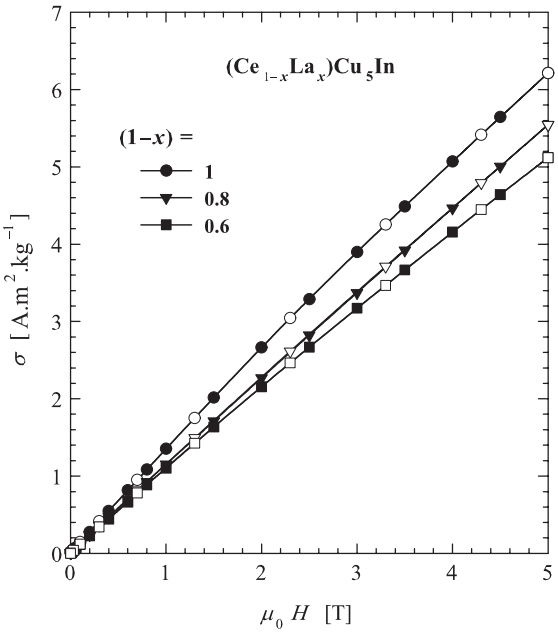

Figure 4. The magnetization σ as a function of the applied field $\mu_0 H$ for $(Ce_{1-x}La_x)Cu_5In$ alloys with $1 - x = 0.6$, 0.8 and 1 measured at 1.7 K. Open symbols correspond to increasing fields and closed symbols to decreasing fields.

Table 2. Magnetic parameters obtained from an LSQ fit of the Curie–Weiss relation (4) against the susceptibility data of different $(Ce_{1-x}La_x)Cu_5In$ alloys.

Ce content $(1 - x)$	θ_p (K)	μ_{eff} (μ_B)
1	−43(1)	2.65(1)
0.9	−57(1)	2.54(1)
0.8	−45(1)	2.58(1)
0.6	−73(1)	2.67(1)
0.2	−35(1)	2.67(1)

Curie–Weiss relation

$$\chi(T) = \frac{N_A \mu_{\text{eff}}^2}{3k_B(T - \theta_p)}. \tag{4}$$

LSQ fits of (4) against the experimental data in the temperature range 100–300 K are shown as solid lines in figure 5. Parameters obtained from these fits, as well as from fits for data of alloys not depicted in figure 5, are given table 2. The effective magnetic moment values obtained across the series are in fair agreement with the value of 2.54 μ_B that corresponds to a free Ce^{3+} ion. Values of the paramagnetic Curie temperature θ_p vary in an irregular manner across the alloy series, whereas one would expect for Ce Kondo systems that $|\theta_p| \sim T_K$ should decrease monotonically with increase in La concentration and hence unit cell volume. This anomalous result is likely due to different degrees of preferred crystallite orientation in the different alloy samples. It is known that the susceptibility of the parent compound $CeCu_5In$ as measured on a single crystal is anisotropic [7], and this could lead to anomalies in the $|\theta_p(x)|$ behaviour if the polycrystalline samples differ in the alignment of anisotropic grains.

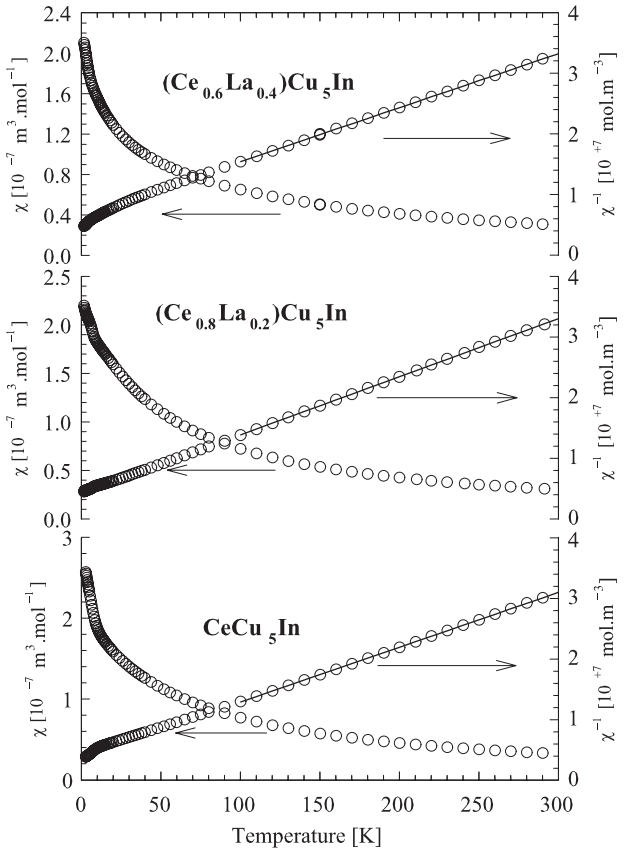

Figure 5. The temperature dependences of the magnetic susceptibility $\chi(T)$ as well as the inverse susceptibility $\chi^{-1}(T)$ of $(Ce_{1-x}La_x)Cu_5In$ alloys with $1 - x = 0.6$, 0.8 and 1. The solid curves are obtained from LSQ fits of the Curie–Weiss relation (4) to the data.

At low temperature the $\chi^{-1}(T)$ curves deviate from Curie–Weiss behaviour, which suggests a depopulation of the excited crystal-field levels associated with the $4f^1$ Ce ion.

For $CeCu_5In$, as well as for the La-substituted alloys, no evidence was found in this study for magnetic ordering down to the lowest temperature of 1.7 K used in the susceptibility measurements. It is noted that antiferromagnetic order has been reported for the $CeCu_{6-x}In_x$ alloys at $T_N = 2.2$ K for $x = 1.5$ and $T_N = 1.5$ K for $x = 1.75$. Hence the possibility of magnetic order at lower temperatures than used in this investigation cannot be excluded for the $(Ce_{1-x}La_x)Cu_5In$ alloy system.

3.4. Resistivity

Measurements of $\rho(T)$ were made on both as-cast and annealed $(Ce_{1-x}La_x)Cu_5In$ alloy samples. Some samples benefitted from annealing since their room-temperature and 4 K resistivity values were reduced relative to that of the as-cast samples. The largest such effect was found for the parent compound, for which $R = \rho(295\text{ K})/\rho(4\text{ K})$ of the annealed sample takes a value of 2.15 compared to $R = 1.23$ of the as-cast sample. However, for several of the alloy samples (e.g. for $x = 0.3$, 0.5, 0.7) the observed $\rho(295\text{ K})$ values of the annealed samples were up to two times larger than for the corresponding as-cast samples. It was furthermore

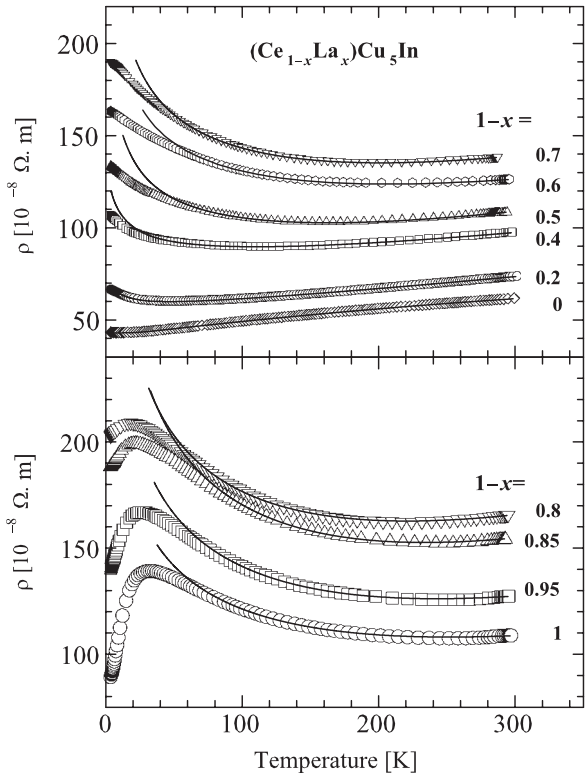

Figure 6. Temperature dependence of the electrical resistivity in the temperature range $4 \leqslant T \leqslant 300$ K for alloys in the system $(Ce_{1-x}La_x)Cu_5In$. The solid lines are LSQ fits of (6) to the measured data. The calculated parameters ρ_0', C_K and κ are given in table 3. Note that depopulated data sets (plotting 1 point out of 5) are plotted in this figure in order to facilitate comparison with the fitted line. The full data sets have been used for LSQ fits.

observed that the $\rho(T)$ curves of the annealed samples lacked the systematic concentration-dependent evolution compared to what was found for the as-cast samples. It was noted that annealing resulted in brittleness of the samples, and it is thought that the spurious behaviour of the annealed alloys may originate from microcracks introduced by annealing. For this reason we present measurements of $\rho(T)$ in this paper on as-cast alloys only, and these are depicted in figure 6.

It is seen in figure 6 that alloys with $0.8 \leqslant (1-x) \leqslant 1$ exhibit coherent Kondo behaviour at low temperatures. A maximum in $\rho(T)$ is observed at temperatures T_m^ρ for these alloys, as given in table 3. At higher temperatures for all Ce-containing alloys in the series, $\rho(T) \sim -\ln(T)$, as is to be expected for incoherent Kondo scattering.

In order to describe the $\rho(T)$ behaviour of the alloy series, first consider the results for the non-magnetic reference compound $LaCu_5In$. It is observed in figure 6 that there is a departure from the approximately linear $\rho(T)$ behaviour one would expect at higher temperatures from the Bloch–Grüneisen description [19]. It turns out that the results are rather described by the so-called Bloch–Grüneisen–Mott formula

$$\rho(T) = \rho_0 + \frac{4\kappa}{\theta_R}\left(\frac{T}{\theta_R}\right)^5 \int_0^{\theta_R/T} \frac{x^5\,\mathrm{d}x}{(\mathrm{e}^x - 1)(1 - \mathrm{e}^{-x})} - \alpha T^3 \tag{5}$$

Table 3. Parameters ρ_0' and C_K describing the resistivity of the $(Ce_{1-x}La_x)Cu_5In$ system in the incoherent region and the coefficient κ of the contribution of electron–phonon scattering to the resistivity. The temperature values of T_m^ρ, where a maximum in the resistivity is observed for dense Kondo alloys, and of T_m^s, where the thermoelectric power exhibits a maximum, are also given.

Ce content $(1-x)$	ρ_0' (10^{-8} Ω m)	C_K (10^{-8} Ω m)	κ (10^{-7} Ω m K)	T_m^ρ (K)	T_m^s (K)
1	245.8(4)	43.3(1)	373(6)	33.0(5)	46(2)
0.95	305.2(7)	53.7(1)	482(7)	26.4(5)	
0.85	375.7(9)	66.0(3)	627(9)	21.7(5)	
0.8	341.7(6)	60.2(1)	588(8)	19.0(5)	50(2)
0.7	244.7(2)	43.22(4)	463(7)		
0.6	202.1(3)	35.9(1)	375(5)		52(2)
0.5	146.1(2)	25.69(3)	338(4)		49(2)
0.4	69.0(1)	12.13(3)	226(3)		47(3)
0.2	26.78(4)	4.69(1)	185(3)		

where ρ_0 originates from the scattering of conduction electrons from defects, the second term is the conventional electron–phonon scattering contribution and the last term is included to account for the interband scattering [20] of the conduction electrons. An LSQ fit of (5) to the experimental data for $LaCu_5In$ gives the solid curve in figure 6 and yields $\rho_0 = 43(1)\times10^{-8}\,\Omega\,m$, $\kappa = 158(2)\times10^{-7}\,\Omega\,m\,K$, $\theta_R = 149(1)\,K$ and $\alpha = 9(1)\times10^{-16}\,\Omega\,m\,K^{-3}$.

The $\rho(T)$ curves for compositions and temperatures where incoherent Kondo scattering is observed may be described by

$$\rho(T) = \rho_0' + \rho_{ph} - C_K \ln(T) \tag{6}$$

where ρ_0' includes, in addition to the electron–defect scattering component ρ_0, a large temperature-independent spin-disorder component [21], and possibly a Nordheim-like contribution resulting from atomic disorder due to the presence of two kinds of atoms (Ce, La) in the $CeCu_5In$ Kondo lattice [22]. It is observed that, upon doping of $LaCu_5In$ with 20% Ce or more, the resistivity above 150 K is linear in T. Thus it appears that the interband scattering that seems to be present for $LaCu_5In$ is suppressed with 20% Ce doping. For this reason we include only the Bloch–Grüneisen term (second term in (5)) in ρ_{ph} in (6). Furthermore, the value of the resistivity Debye temperature $\theta_R = 149$ K obtained for $LaCu_5In$ was used in analysing the results of the other alloys. Since the values of the atomic mass of Ce and La are nearly the same, the lattice vibrational spectra of these alloys and hence θ_R are expected to be similar. LSQ fits of (6) to the experimental data for the temperature region where incoherent Kondo scattering is found for the various alloys give the solid curves in figure 6. Values of the fit parameters ρ_0', C_K and κ are given in table 3.

3.5. Magnetoresistivity

Magnetoresistivity (MR) measurements were made on a selected number of $(Ce_{1-x}La_x)Cu_5In$ alloys for which their $\rho(T)$ curves are characteristic of single-ion incoherent Kondo scattering. Measurements were performed on as-cast samples in transverse magnetic fields up to 8 T and at various temperatures between 1.5 and 28 K. Figure 7 gives the isothermal MR of a representative alloy, namely $(Ce_{0.5}La_{0.5})Cu_5In$. For all the investigated alloys ($1-x = 0.2, 0.3, 0.5$ and 0.6) a negative MR has been observed at all temperatures as a result of suppression of the incoherent Kondo scattering in a magnetic field. The result of the Bethe

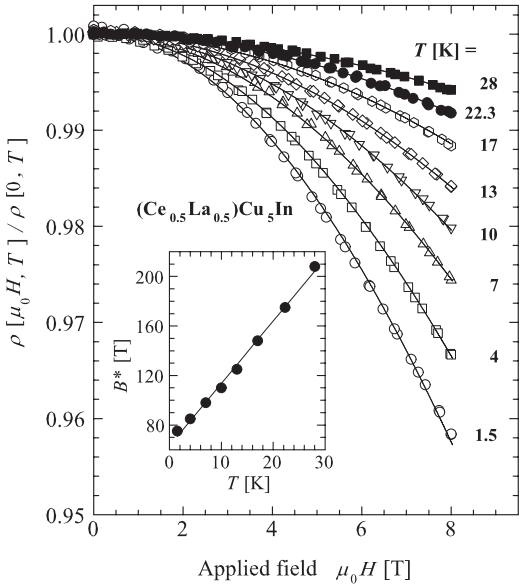

Figure 7. The magnetic field dependence of the electrical resistivity at a number of sample temperatures for the alloy $(Ce_{0.5}La_{0.5})Cu_5In$. The data have been measured in increasing and decreasing fields without evidence of hysteresis. The solid curves in the main figure are LSQ fits of the Bethe ansatz theory of magnetoresistivity (7) to the experimental data. The inset shows the temperature variation of the characteristic field $B^*(T)$, and the solid curve through the data points is an LSQ fit of (8) to the B^* values.

ansatz calculations of the Coqblin–Schrieffer model given by Andrei [23] and Schlottmann [24]

$$\frac{\rho(\mu_0 H)}{\rho(\mu_0 H = 0)} = \left[\frac{1}{2j+1}\sin^2\left(\frac{\pi n_f}{2j+1}\right)\sum_{\ell=0}^{2j}\sin^{-2}(\pi n_\ell)\right]^{-1} \tag{7}$$

yields an exact solution for the spin-$\frac{1}{2}$ case. It is considered appropriate to use the spin-$\frac{1}{2}$ result for a description of our MR results, notwithstanding that the Ce^{3+} ion has $j = \frac{5}{2}$, since the crystal electric field for orthorhombic symmetry results in an effective $j = \frac{1}{2}$ moment for the low temperature ground state [21]. $\rho(\mu_0 H)/\rho(\mu_0 H = 0)$ is determined by a characteristic field B^* which has the following temperature dependence [25]:

$$B^*(T) = B^*(0) + \left(\frac{k_B T}{g\mu_K}\right) = \frac{k_B(T_K + T)}{g\mu_K}. \tag{8}$$

LSQ fits of (7) to the experimental MR data give values of $B^*(T)$ as depicted in the inset to figure 7. An LSQ fit of (8) to these B^* values yields the value of $B^*(0)$, hence of T_K and the magnetic moment μ_K of the Kondo ion. Values of T_K and μ_K from the MR analyses are given in table 4. The values of the magnetic moment μ_K observed for the Kondo ion are considerably reduced from the free-ion value. A value of $g = 2$ corresponding to the spin-$\frac{1}{2}$ case used in our MR fits was used to calculate μ_K. It is noted that once $B^*(T)$ have been determined, the calculation of T_K using (8) is independent of the particular choice of g. Finally, we illustrate in figure 8 for one of the alloys the excellent scaling of the MR data in accord with the Bethe ansatz formulation of the single-ion magnetoresistivity by showing the collapse of MR data from all isotherms on a single curve in a plot of $\rho(\mu_0 H, T)/\rho(0, T)$ versus $\mu_0 H/B^*(T)$. A similar scaling of the MR data was observed for all of the investigated alloys.

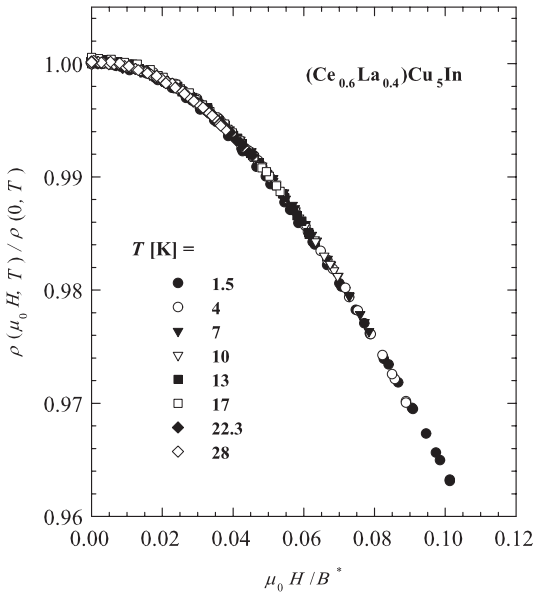

Figure 8. Magnetoresistivity data for different isotherms of $(Ce_{0.6}La_{0.4})Cu_5In$ as measured in fields up to 8 T and at various temperatures between 1.5 and 28 K are shown to scale well with the Bethe ansatz formulation of the single-ion magnetoresistivity.

Table 4. Values of the Kondo temperature T_K and the magnetic moment of the Kondo ion μ_K as obtained from a fit of (7) and (8) to the magnetoresistivity data of several $(Ce_{1-x}La_x)Cu_5In$ alloys.

Ce concentration $(1-x)$	0.6	0.5	0.3	0.2
T_K (K)	13.9(8)	12.5(7)	7.6(8)	4.5(7)
μ_K (μ_B)	0.151(4)	0.148(4)	0.106(4)	0.056(3)

3.6. Thermoelectric power

Thermoelectric power $S(T)$ measurements are displayed in figure 9 for annealed samples of $CeCu_5In$ and several $(Ce_{1-x}La_x)Cu_5In$ alloys. Within the investigated temperature range all these exhibit positive values of $S(T)$ and a single maximum occurring at temperatures T_m^s, as given in table 3. The observed maximum value of $S = 48\ \mu V\ K^{-1}$ at $T_m^s = 46$ K for our polycrystalline $CeCu_5In$ sample is very similar to maxima values of $S = 52\ \mu V\ K^{-1}$ for the a axis and $S = 46\ \mu V\ K^{-1}$ for the b axis of a $CeCu_6$ crystal occurring at a temperature $T_m^s = 40$ K [26]. Upon substitution of Ce with La, the observed $S(T)$ is reduced, but the occurrence of a maximum is retained in all alloys with the temperature T_m^s rather independent of x, as seen in figure 9. In this respect the behaviour of $S(T)$ is different from that of $\rho(T)$ for our system in that the temperature T_m^ρ where a maximum appears in $\rho(T)$ diminishes significantly with La substitution, as is evident from table 3. The location of the resistance maximum, which is a precursor of the coherence that sets in at a lower temperature, is probably a fair indication of the Kondo temperature ($T_K \sim T_m^\rho$) for this system, for which $\rho(T)$ in the coherent region is characterized by a single maximum. The maxima in $S(T)$ occurring for the various $(Ce_{1-x}La_x)Cu_5In$ alloys at temperatures T_m^s indicated by arrows in figure 9 are approximately independent of x. These maxima are considered to originate from the combined effect of the crystalline electric field and Kondo behaviour [27, 28].

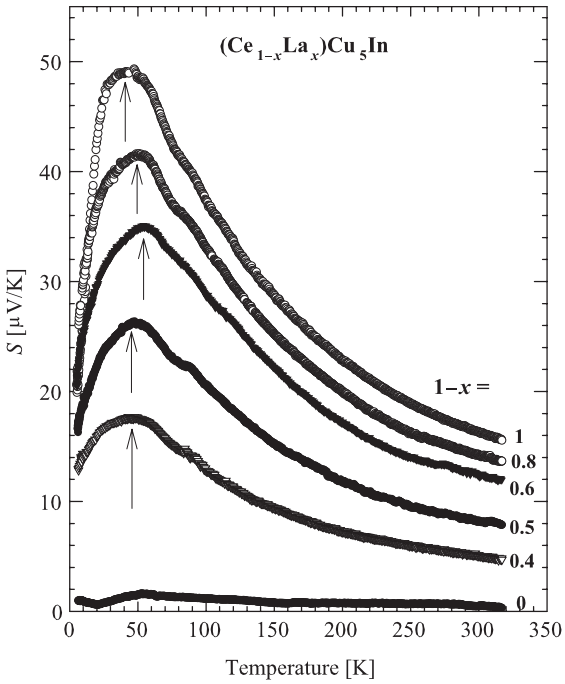

Figure 9. The thermoelectric power S versus temperature for various $(Ce_{1-x}La_{1-x})Cu_5In$ alloys. The arrows indicate the position of a maximum in $S(T)$.

Finally, it is noted that in the case of $CeCu_6$ there is a shoulder at about 5 K in addition to the maximum which appears at $S(T)$. Upon La substitution, the maximum at higher temperatures is retained even for a Ce concentration of 9.4%, while the shoulder develops into a peak that occurs around 3.5–5 K depending on the Ce content [29]. Such details have not been observed in our study, which was limited to a lowest temperature of 5 K.

3.7. The volume dependence of T_K

The variation of the Kondo temperature with substitution of La for Ce in Ce compounds, $T_K(x)$, has often been described in terms of the compressible Kondo lattice model [10]

$$T_K(x) = T_K(x=0)\exp\left[\frac{q\,[V(x)-V_0]}{V_0|J\,N(E_F)|_{x=0}}\right]. \tag{9}$$

$V(x)$ and V_0 are the volumes of the unit cell for the La-doped alloy and the Ce parent compound respectively, J is the on-site Kondo interaction, $N(E_F)$ is the density of states at the Fermi level, and q takes on values between 6 and 8. We interpret our results in terms of (9) by assuming that for the dense Kondo alloys their maxima in $\rho(T)$ occurring at T_m^ρ are a fair indication of the Kondo temperature T_K. It is observed from figure 6 and table 3 that these T_m^ρ values decrease monotonically with decreasing Ce concentration. This is also true for the T_K values derived from MR measurements. It is further noted that using $T_K = 0.206\pi^2 R/3\gamma$ as derived by Oliveira and Wilkins [30] leads to $T_K = 27.4$ K for $CeCu_5In$ using $\gamma^{conv} = 205$ mJ mol^{-1} K^{-2} from section 3.2.

A plot of $T_m^\rho(x)$ and of the magnetoresistivity derived $T_K(x)$ values against $[V(x)-V_0]/V_0$ as obtained from our x-ray measurements is given in figure 10. Both data sets show a smooth

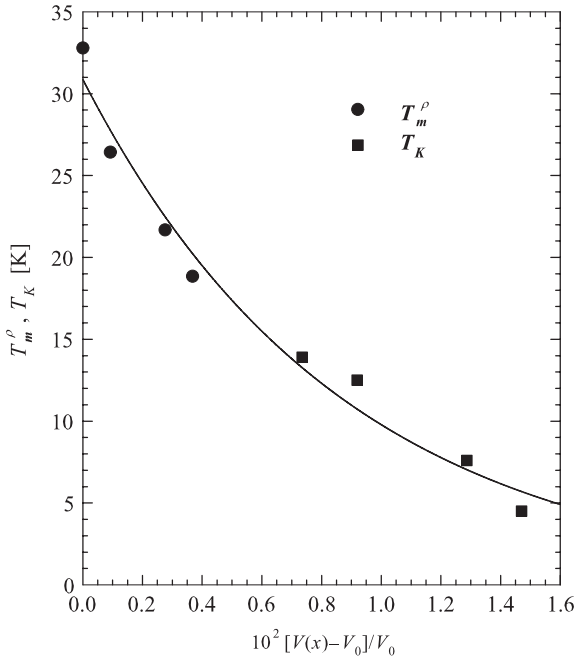

Figure 10. A plot of T_m^ρ as well as T_K values derived from the magnetoresistivity versus $(V(x) - V_0)/V_0$ as obtained from our x-ray measurements. The solid curve is an LSQ fit of (9) to the T_m^ρ and T_K values.

decrease with volume increase. An LSQ fit of (9) to the combined data sets gives the solid line. Using $q = 6$, the analysis gives $|JN(E_F)| = 0.052(4)$ for $CeCu_5In$, which may be compared with a value of 0.09 obtained for $CeCu_6$ [31].

The smooth variation of T_m^ρ and T_K with x through the alloy series is in contrast to the irregular manner in which θ_p varies with x as reported in section 3.3, where it has been suggested that the irregular θ_p variation could originate from different degrees of preferred crystallite orientation in the different alloy samples. It may be questioned why such effects were not observed for the T_m^ρ and T_K values derived from $\rho(T)$ and MR studies. It is noted that the latter measurements were made on significantly larger specimens which were always cut parallel to the bottom and from the central part of the button-shaped samples. It is likely that the effect of different crystallite compositions averages out more effectively for the much larger resistivity specimens, compared to the magnetization specimens.

4. Conclusion

This study confirms that $CeCu_5In$ exhibits dense Kondo properties with an enhanced specific heat at low temperatures, and a Kondo temperature which is appreciably higher than that of $CeCu_6$ ($T_K \approx 3$ K). Electrical resistivity measurements clearly illustrate the evolution from dense Kondo to incoherent single-ion Kondo behaviour. Susceptibility measurements at higher temperatures (100–300 K) give effective magnetic moments in fair agreement with the Ce^{3+} value. Results of magnetoresistance measurements on selected $(Ce_{1-x}La_x)Cu_5In$ alloys conform with the Bethe ansatz description of this property, and are used to obtain $T_K(x)$ values. These, together with values of T_m^ρ (the temperature at which a maximum occurs for

the coherent dense Kondo alloys), are used in a compressible Kondo lattice description of the system. The thermoelectric power, which is positive for all the $(Ce_{1-x}La_x)Cu_5In$ alloys, is likely to be understood in terms of the combined effects of the crystalline electric field and the Kondo behaviour.

Acknowledgments

Support by the South African National Research Foundation (NRF) through grant GUN 2053778, the Research Division of the University of the Witwatersrand and the Polish State Committee for Scientific Research (KBN) through grant 4T08A 045 24 is acknowledged. Any opinion, findings or conclusions expressed in this paper are those of the authors and do not necessarily reflect the views of the NRF.

References

[1] Bauer E 1991 *Adv. Phys.* **40** 417
[2] See references contained in Strydom A M and du Plessis P de V 1999 *J. Phys.: Condens. Matter* **11** 2285
[3] von Löhneysen H 1995 *Physica* B **206/207** 101
[4] Ott H R, Rudigier H, Fisk Z, Willis J O and Stewart G R 1985 *Solid State Commun.* **55** 235
[5] Amato A, Jaccard D, Walker E and Flouquet J 1985 *Solid State Commun.* **55** 1131
[6] Sumiyama A, Oda Y, Nagano H, Ōnuki Y, Shibutani K and Komatsubara T 1986 *J. Phys. Soc. Japan* **55** 1294
[7] Kasaya M, Satoh N, Miyazaki T and Kumazaki H 1995 *Physica* B **206/207** 314
[8] Kaczorowski D, Kalychak Ya M and Zaremba V I 2000 *Acta Phys. Pol.* A **97** 189
[9] Tchoula Tchokonté M B, Kaczorowski D, du Plessis P de V and Strydom A M 1999 *Physica* B **259–261** 22
[10] Lavagna M, Lacroix C and Cyrot M 1983 *J. Phys. F: Met. Phys.* **13** 1007
[11] Holland T J B and Redfern S A T 1997 *Mineral. Mag.* **61** 65
[12] Henkie Z, Markowski P J, Wojakowski A and Laurent Ch 1987 *J. Phys. E: Sci. Instrum.* **20** 40
[13] Wawryk R and Henkie Z 2001 *Phil. Mag.* B **81** 223
[14] Stewart G R 1984 *Rev. Mod. Phys.* **56** 755
[15] Stewart G R, Fisk Z, Willis J O and Smith J L 1984 *Phys. Rev. Lett.* **52** 679
[16] Doniach S and Engelsberg S 1966 *Phys. Rev. Lett.* **17** 750
[17] Trainor R J, Brodsky M B and Culbert H V 1975 *Phys. Rev. Lett.* **34** 1019
[18] Stewart G R, Giorgi A L, Brandt B L, Foner S and Arko A J 1983 *Phys. Rev.* B **28** 1524
[19] Mott N F and Jones H 1958 *The Theory of the Properties of Metals and Alloys* (Oxford: Oxford University Press)
Grimvall G 1981 *The Electron–Phonon Interaction in Metals* (Amsterdam: North-Holland)
[20] Mott N F 1936 *Proc. R. Soc.* **156** 368
Jones H 1956 *Handbuch der Physik* vol 19 (Berlin: Springer)
[21] Cornut B and Coqblin B 1972 *Phys. Rev.* B **5** 4541
[22] Sumiyama A, Oda Y, Nagano H, Ōnuki Y, Shibutani K and Komatsubara T 1986 *J. Phys. Soc. Japan* **55** 1294 illustrated the presence of such a contribution for the $(Ce_{1-x}La_x)Cu_6$ system
[23] Andrei N 1982 *Phys. Lett.* A **87** 299
[24] Schlottmann P 1983 *Z. Phys.* B **51** 223
[25] Batlogg B, Bishop D J, Bucher E, Golding B Jr, Raminez A P, Fisk Z, Smith J L and Ott H R 1987 *J. Magn. Magn. Mater.* **63/64** 441
[26] Namiki T, Sato H, Urakawa J, Sugawara H, Aoki Y, Settai R and Ōnuki Y 2000 *Physica* B **281/282** 359
[27] Bhattacharjee A K and Coqblin B 1976 *Phys. Rev.* B **13** 3441
[28] Fischer K H 1989 *Z. Phys.* B **76** 315
[29] Ōnuki Y and Komatsubara T 1987 *J. Magn. Magn. Mater.* **63/64** 281
[30] Oliveira L N and Wilkins J W 1981 *Phys. Rev. Lett.* **47** 1553
[31] Kagayama T and Oomi G 1993 *Transport and Thermal Properties of f-Electron Systems* ed G Oomi *et al* (New York: Plenum) p 115